Organometallics 1990, *9*, 2223-2233

Molecular Orbital Study of Olefin Homologation by Bimetallic Complexes. 2. The Elimination Step

Françoise Delbecq

Institut de Recherches sur la Catalyse, 2, avenue A. Einstein, 69626 Villeurbanne Cêdex, France

Received September 8, 1989

The formation of propene from a diferracyclopentane is studied on the basis of molecular orbital arguments founded on extended Hückel theory calculations. Several reaction paths are compared. If the CO dissociation is easy, this path followed by a β-hydride elimination to give the dinuclear hydrido-alkyl complex $Fe(CO)_3HFe(CO)_4(C_3H_5)$ is preferred. As the dinuclear elimination is difficult, the products are more easily obtained by a mononuclear elimination from a cis hydrido-alkyl complex. The latter complex comes from a fluxional migration of the hydride. If CO loss is difficult, the formation of cyclopropane can compete with that of propene.

I. Introduction

In our first report on the subject,[1] we studied how a bridged methylene complex and ethylene are transformed into a dimetallacyclopentane (eq 1). Such an intermediate had been postulated in olefin homologation by Pettit[2] for a diiron complex, by Norton[3] for a diosmium complex, and by Bergman for a dicobalt complex.[4a] These three isoelectronic complexes (d^7, 18 electrons) all evolve into propene and a metallic residue upon heating in benzene or toluene, thus effectively transforming ethylene to propene[2-4] (eq 2).

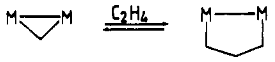

(1)

M= Fe(CO)$_4$, Os(CO)$_4$ or Co(η^5-C$_5$H$_5$)CO

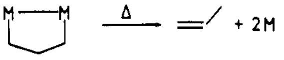

(2)

In the presence of ethylene, the metallic residue is isolated as the stable ethylene complex $Fe(CO)_4(C_2H_4)$ or $Co(C_5H_5)CO(C_2H_4)$. The purpose of the present work is to study several possible pathways for the decomposition of the dimetallacyclopentane (eq 2). As in the previous paper, we chose the diiron complex I (M = Fe) (see Scheme I). Our analysis is based on extended Hückel calculations.[5]

Let us first summarize the various possibilities. The formation of propene from the carbon chain requires the migration of one central hydrogen. The first mechanism has been suggested by Pettit[2] and Bergman:[4] after CO dissociation a β-hydride elimination occurs, giving an olefin π-complex (path a of Scheme I). Then a dinuclear [1 - 2] reductive elimination leads to the products. However, such a path might not be favorable, since previous calculations have shown that the latter reaction is intrinsically symmetry forbidden.[6] In fact, Norton et al. have found that the d^7 18e compound $Os(CO)_4HOs(CO)_4CH_3$ does not undergo an intramolecular reductive elimination of methane at 50 °C[7] and diosmacyclopentane (eq 2, M = $Os(CO)_4$) decomposes only at 130 °C.[3]

Scheme I

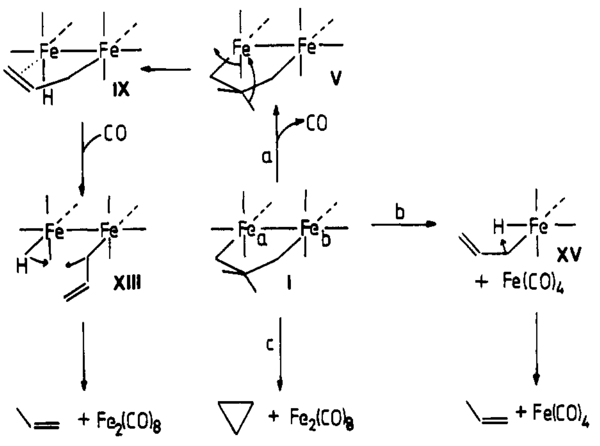

Scheme II

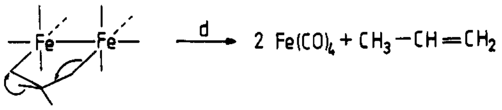

Furthermore, the hypothesis of CO dissociation can also be questioned. First of all, the thermal decomposition of iron or osmium carbonyl compounds can require a temperature higher (>100 °C)[8] than the temperature of the reaction under discussion. In the case of the dicobalt complex $Co_2(CO)_2Cp_2(C_3H_6)$, it has been shown that the loss of CO is rather difficult and must be initiated by $CpCo(C_2H_4)$.[4] In this case, propene is obtained. When no initiation occurs, the temperature must be high (100 °C) to obtain the loss of CO and the formation of a second product (cyclopropane) becomes competitive (propene to cyclopropane ratio 4:1). When the temperature is lower (56 °C), the loss of CO is inhibited and only cyclopropane is obtained. In fact, in all reactions studied[2-4] cyclopropane exists as a minor product. Therefore, the formation of propene and of cyclopropane seem to be competitive and to depend on the experimental conditions. This assumption is supported by the work of Knox et al.[9] on the gen-

---

[1] Part 1: Bigot, B.; Delbecq, F. *Organometallics* **1987**, *6*, 172-180.

[2] Summer, C. E., Jr.; Riley, P. E.; Davis, R. E.; Pettit, R. *J. Am. Chem. Soc.* **1980**, *102*, 1752-1754.

[3] Motyl, K. M.; Norton, J. R.; Schauer, C. K.; Anderson, O. P. *J. Am. Chem. Soc.* **1982**, *104*, 7325-7327.

[4] (a) Theopold, K. H.; Bergman, R. G. *J. Am. Chem. Soc.* **1981**, *103*, 2489-2491. (b) *J. Am. Chem. Soc.* **1980**, *102*, 5694-5695.

[5] Hoffmann, R. *J. Chem. Phys.* **1963**, *39*, 1397.

[6] Trinquier, G.; Hoffmann, R. *Organometallics* **1984**, *3*, 370-380.

[7] Okrasinski, S. J.; Norton, J. R. *J. Am. Chem. Soc.* **1977**, *99*, 295-297.

[8] *Comprehensive Organometallic Chemistry*; Wilkinson, G., Ed.; Pergamon Press: Oxford, U.K., 1982; Vol. IV, pp 243, 968.

[9] Cooke, M.; Forrow, N. J.; Knox, S. A. R. *J. Chem. Soc., Dalton Trans.* **1983**, 2435-2440.

0276-7333/90/2309-2223$02.50/0

eration of hydrocarbons from methylene chains linking two metal centers through intermediates thought to be dimetallacyclic: by photolysis (loss of CO) propene is obtained, and by thermolysis (no CO loss) cyclopropane is preferred. For all these reasons, mechanisms other than that of Pettit have been investigated. The first one (without CO dissociation) involves Fe–C and Fe–Fe bond cleavages simultaneous with the H migration, as in a substitution reaction (path b of scheme I). This pathway is interesting in that it leads to a monometallic cis hydrido–alkyl complex that can evolve into propene by a mononuclear reductive elimination. This latter reaction has been shown to be symmetry allowed for planar d^8 complexes.[10]

The second mechanism is the formation of cyclopropane (path c). Finally, a [1 - 2] sigmatropic migration of a central hydrogen on the adjacent carbon with a simultaneous cleavage of the Fe–C bonds can lead directly to the products (path d, Scheme II).

II. Prior Dissociation of CO, β-Hydride Elimination, and Dinuclear Reductive Elimination (Path a)

(a) CO Dissociation. We will first discuss which CO dissociates the most easily. Each iron atom has an octahedral environment (II). The Fe–CO overlap populations

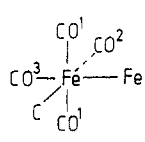

II

(op) reveal the existence of three sorts of carbonyls: the two apical CO's (op = 0.82), the basal CO^2 trans to the Fe–C bond (op = 0.78), and the basal CO^3 trans to the Fe–Fe bond (op = 0.76). Thus, the CO trans to Fe is less tightly bound and is likely to dissociate more easily. Let us now explain this result. The three possible complexes obtained by CO dissociation are III–V.

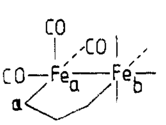

III

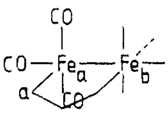

IV

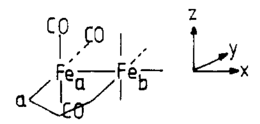

V

Each of the complexes has one metal in a square-planar pyramidal environment. It has already been shown that a d^7 five-coordinate molecule prefers such a structure over that of a trigonal pyramid.[11] The LUMO of each complex is hybridized toward the empty site. For IV it is delocalized over C_a and for V over Fe_b, whereas for III it is almost exclusively localized on Fe_a (d_{z^2}). This is explained by the relative order of the interacting orbital of the ligands trans to the empty site (the carbon chain, the other iron atom, and a CO, respectively). The overlap with an incoming CO is therefore greater in III than in IV or V.

Let us now study the relative stability of the three $Fe_2(CO)_7C_3H_6$ isomers III–V:III and IV are 23 and 14 kcal above V, respectively. Hoffmann et al. have studied the preferred positions of the substituents in the ML_5 complexes.[11a] However, the d^7 case has not been clearly described. Furthermore, in our case two substituents (C_a and Fe_b) coexist whose influence can compete. The complexes III–V can be considered as built up from the $Fe_2(CO)_7$ fragments VI–VIII interacting with the C_3H_6 fragment.

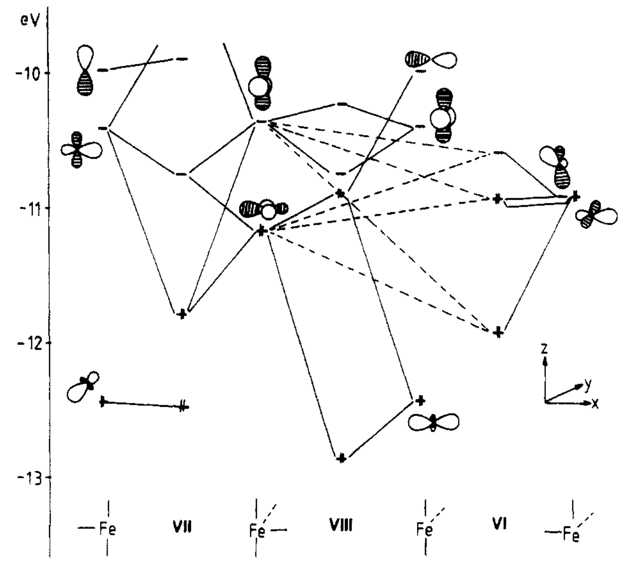

Figure 1. Interaction diagram between $Fe(CO)_3$ and $Fe(CO)_4$ fragments.

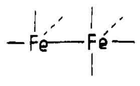

VI

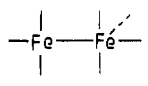

VII

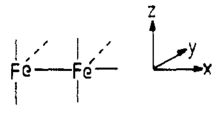

VIII

Each $Fe_2(CO)_7$ fragment itself comes from the interaction of a $Fe(CO)_3$ and a $Fe(CO)_4$ fragment. The orbitals of these fragments have already been described,[12] and their interaction diagrams are given in Figure 1. In VII and VIII a strong stabilizing HOMO–LUMO interaction exists, but in VIII a supplementary destabilizing HOMO–HOMO interaction occurs. This explains why VIII is less stable than VII by 27 kcal/mol. Concerning VI, the set of degenerate orbitals of the C_{3v} $Fe(CO)_3$ fragment interacts with both the LUMO and the HOMO of $Fe(CO)_4$, giving two high-lying occupied orbitals. Therefore, VI is the least stable isomer (46 kcal/mol above VII). It is worthy of note that the HOMO–LUMO gap in VI and VIII is small: these fragments are unstable toward a Jahn–Teller distortion that leads to the more stable isomer VII.

The interaction of VII and VIII with the C_3H_6 fragment is now considered (VI has been excluded, owing to its much higher energy). The orbitals of the C_3H_6 fragment have already been described.[1] The frontier orbitals are the in-phase (LUMO) and the out-of-phase (HOMO) combinations of the two carbon p orbitals along the *y* axis. In both fragments VII and VIII, the HOMO and the LUMO have coefficients along the *y* axis and therefore overlap with 1 and 2 giving similar interactions. The difference between VII and VIII comes from the existence in VII of an occupied orbital, mainly d_{y^2}, that gives with 2 a destabilizing 4e interaction. The corresponding orbital in VIII is d_{x^2}, which does not overlap with the C_3H_6 orbitals. The foregoing explains why V is more stable than IV even

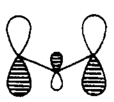

1 LUMO

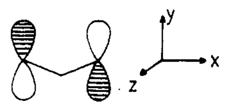

2 HOMO

---

[10] Hoffmann, R. In *IUPAC Frontiers of Chemistry*; Laidler, K. J., Ed.; Pergamon Press: Oxford, U.K., 1982; pp 247–263. Tatsumi, K.; Hoffmann, R.; Yamamoto, A.; Stille, J. K. *Bull. Chem. Soc. Jpn.* **1981**, *54*, 1857–1867.

[11] (a) Rossi, A.; Hoffmann, R. *Inorg. Chem.* **1975**, *14*, 365–374. (b) Elian, M.; Hoffmann, R. *Inorg. Chem.* **1975**, *14*, 1058–1076.

[12] Albright, T. A. *Tetrahedron* **1982**, *38*, 1339–1388.

Chart I

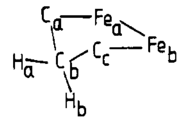

though VIII is less stable than VII.

In conclusion, the easiest dissociation of CO leads to the most stable $Fe_2(CO)_7C_3H_6$ complex V. The dissociation requires 2.6 eV (60 kcal/mol). A similar value is found by Hoffmann.[13] Few experimental values are available: the average bond dissociation energy has been found to be 1.25 eV in $Fe(CO)_5$.[14] However, the dissociation energy of the first CO in $Fe(CO)_5$ has been shown to be 2.4 eV (55 kcal/mol)[15a] or 1.8 eV (41.5 kcal/mol).[15b] On the other hand, the complex $Fe_2(CO)_8(\mu\text{-}PR_2)$ easily loses one CO at room temperature.[15c] Thus, the ease of the CO dissociation depends on the complex.

(b) β-Hydride Elimination. The β-hydride elimination of metal alkyls is a well-known reaction in organometallic chemistry. It has been shown experimentally that it requires a metal complex which is coordinatively unsaturated or contains labile ligands.[16] Further, it is a cis elimination, the metal and the hydride being cis relative to the C–C bond.[17] This reaction and its reverse, the olefin insertion reaction, have been studied theoretically.[18,19] Hoffmann showed,[18] with the extended Hückel theory (EHT) method, that the metal, the hydride, and the C–C bond must be coplanar. From ab initio calculations,[19] Morokuma concluded that the β-hydride elimination is easier if there is an agostic interaction between the metal and the hydride. Both studies have been carried out with the set Ni, Pd, Pt.

From a geometrical point of view, the best isomer for the β-hydride elimination is III. It is worthy of note that it is the least stable. The studied system is a five-membered metallacycle whose geometry is given in ref 1. As we can see in Chart I, the C_b–H_a bond is in the FeCC plane but is trans to the metal. The C_b–H_b bond, which is directed toward the metal, is almost perpendicular to the FeCC plane so that the required coplanar orientation cannot be achieved easily. It has been shown experimentally[20] that, owing to these geometrical constraints, some five-membered metallacycles are relatively stable toward the β-hydride elimination and decompose by different mechanisms. Therefore, the complex studied here does not seem very favorable to the β-hydride elimination. It is however interesting to note that there exist in III two low-lying orbitals, the in-phase and out-of-phase combinations of the Fe d_{z^2} orbitals, that mixt weakly with the $\sigma_{C_bH_b}$ orbital in a bonding way. Now the d_{z^2} orbital is mainly the vacant orbital of the complex. This would signify that a kind of agostic interaction exists between H_b and Fe_a. However, owing to the steric constraints, it cannot bring H_b and Fe_a nearer.

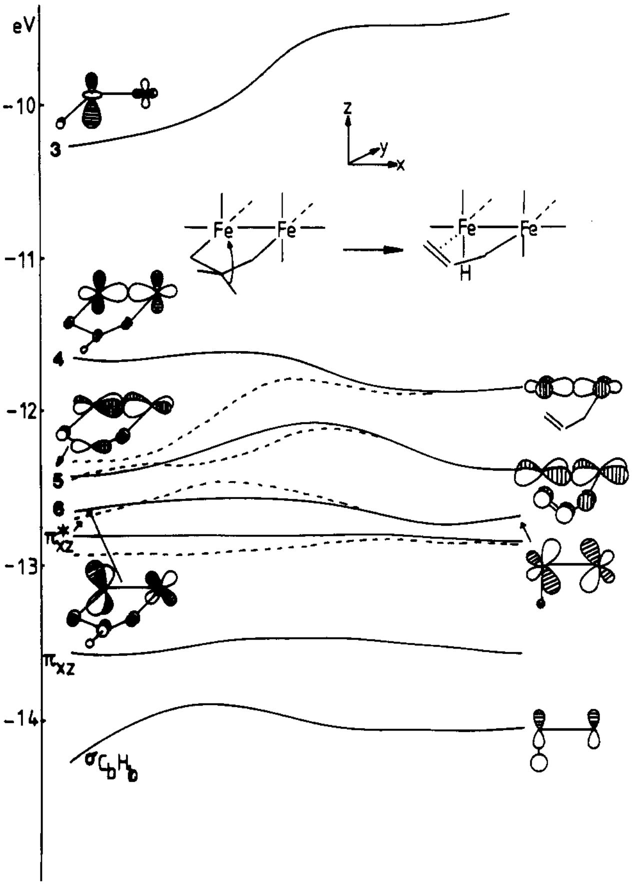

Figure 2. Evolution of the main orbitals during the transformation of III into IX (solid lines) and of V into IX (dashed lines).

Let us consider now the olefin π-complex IX, the product of this elimination. Around Fe_a, we have an

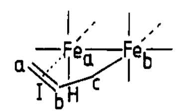

IX

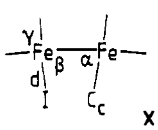

X

olefin–ML_5 complex. In such complexes, the olefin has been shown to be parallel to one axis of the octahedron.[21] The cyclic nature of our system introduces constraints that prevent this geometry. Maintaining the $C_aC_bC_c$ angle at 120°, we have varied the bond angles α and β (see X) and the torsion angle $Fe_aFe_bC_cC_b$ in order to keep the middle of C_aC_b (point I) in the $Fe_aFe_bC_c$ plane. The best values found are $\alpha = 79.35°$ and $\beta = 81.68°$ for Fe_a–Fe_b = 2.7 Å and C_a–C_b = 1.42 Å. This induces a distance Fe_a–I of 2.52 Å and an angle of 45° between the C_aC_b bond and the $Fe_aFe_bC_cI$ plane. Furthermore, a better geometry is obtained when the CO's are slightly displaced so that the three angles are equal (γ). What is interesting to note is the angle of 45° between C_aC_b and the $Fe_aFe_bC_cI$ plane. For normal olefin–ML_5 complexes, this geometry is that of the transition state for the olefin rotation. One example of such an orientation exists already in the literature.[22] By X-ray diffraction, a long Fe—C and a short C═C distance were found. Our computations give the same trends: the Fe_a–I distance is 2.52 Å and the C_a–C_b bond is 1.42 Å instead of 2.12 and 1.46 Å, respectively, in $Fe(CO)_4C_2H_4$.[23]

---

(13) Stockis, A.; Hoffmann, R. *J. Am. Chem. Soc.* **1980**, *102*, 2952–2962.

(14) Connor, J. A. *J. Organomet. Chem.* **1975**, *94*, 195.

(15) (a) Engelking, P. C.; Lineberger, W. C. *J. Am. Chem. Soc.* **1979**, *101*, 5569–5573. (b) Lewis, K. E.; Golden, D. M.; Smith, G. P. *J. Am. Chem. Soc.* **1984**, *106*, 3905–3912. (c) Baker, R. T.; Calabrese, J. C.; Krusic, P. J.; Therien, M. J.; Trogler, W. C. *J. Am. Chem. Soc.* **1988**, *110*, 8392–8412.

(16) Reger, D. L.; Culbertson, E. C. *J. Am. Chem. Soc.* **1976**, *98*, 2789–2794; *Inorg. Chem.* **1977**, *16*, 3104–3107.

(17) Heck, R. F. *J. Am. Chem. Soc.* **1969**, *91*, 6707–6714. Murahashi, S. I.; Yamamura, M.; Mita, N. *J. Org. Chem.* **1977**, *42*, 2870–2874.

(18) Thorn, D. L.; Hoffmann, R. *J. Am. Chem. Soc.* **1978**, *100*, 2079–2090.

(19) Koga, N.; Obara, S.; Kitaura, K.; Morokuma, K. *J. Am. Chem. Soc.* **1985**, *107*, 7109–7116.

(20) McDermott, J. X.; White, J. F.; Whitesides, G. M. *J. Am. Chem. Soc.* **1976**, *98*, 6521–6528.

(21) Albright, T. A.; Hoffmann, R.; Thibeault, J. C.; Thorn, D. L. *J. Am. Chem. Soc.* **1979**, *101*, 3801–3812.

(22) Riley, P. E.; Davis, R. E. *Inorg. Chem.* **1975**, *14*, 2507–2513.

From the energetic point of view, IX has been computed to be isoenergetic with V.

Let us now study the reaction path from III to IX by migration of H_b. It is obtained by varying linearly all the geometrical parameters. The system does not possess any symmetry. Therefore, we cannot have level crossings but only avoided crossings between occupied and unoccupied orbitals. The orbital energies along the reaction path are plotted in Figure 2. It appears that the reaction is allowed, because there is no avoided crossing between the HOMO and LUMO. When the reaction proceeds, the C_b–H_a bond (see Chart I) rotates down and the $\sigma_{C_bH_a}$ and $\sigma_{C_bH_b}$ orbitals are no longer separated as they were in I. Two $\pi_{C_bH_aH_b}$ orbitals are obtained. As a consequence, a coefficient appears on H_b (bonding with C_b) in orbitals **3**, **4**, and **6**. This induces an H_b–Fe_a antibonding interaction in **3** and a bonding one in **4**, explaining why **3** rises and **4** decreases when H_b approaches Fe_a: they cannot cross.

Owing to the lack of symmetry, the other orbitals give a sequence of avoided crossings. The most important orbitals that account for the energy barrier are the low-lying $\sigma_{C_bH_b}$ orbital and **6**. When the C_b–H_b bond is elongated, $\sigma_{C_bH_b}$ rises in energy. However, it mixes quickly with the π_{xz} orbital that lies just above. The mixing develops a bonding interaction between H_b and Fe_a d_{xz}, and this orbital becomes the σ_{FeH} orbital.

The rotation around C_b creates in **6** a coefficient on H_b that is bonding with C_b and antibonding with Fe_a: **6** would correlate with an upper FeH antibonding orbital. However, by mixing it transfers these characteristics to **5**, which rises in turn. At the end of the reaction, the three orbitals **4**–**6** mix together, so that **4** and **5** lose their Fe_aH_b bonding character, which remains only in **6**.

Let us see more precisely what happens at the transition state. In order to do that, the complex has been decomposed into the two fragments $Fe_2(CO)_7$ and C_3H_6. The main interaction occurs between the frontier orbitals **7** and **9** of these fragments, which are the $\sigma_{C_bH_b}$ orbital on one hand and the empty Fe_a $d_{z^2-y^2}$ on the other hand. A weak interaction exists also between **8** and a higher unoccupied orbital having mainly Fe_a d_{z^2} character. **7** and **8** are the $\pi_{C_bH_aH_b}$ orbitals cited above. We find here the key to the β-hydride elimination suggested by Morokuma:[19] "it is important that a CH···M interaction takes place, whose origin is the electron-donative interaction from a CH σ bond to a vacant d orbital".

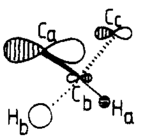

7

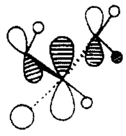

8

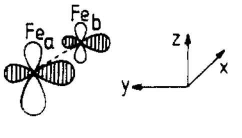

9

The activation energy has been computed to be 1.7 eV. We have just studied the β-elimination from III. As we said before, this is the least stable $Fe_2(CO)_7C_3H_6$ isomer. What is the barrier when we start from isomer V (eq 3)?

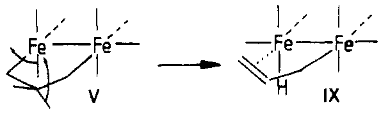

(3)

It has been computed to be 2.3 eV. The reaction coordinates are the same as before, except that the vertical CO rotates to become basal. The difference in the energy barrier comes essentially from the behavior of the π^*_{xz} orbital and of the HOMO (Figure 2, dashed lines). When the vertical CO rotates, its σ orbital interacts more and more with Fe_a d_{xz} and destabilizes it. At the transition state, the angle between CO and the vertical axis is about 45°, the interaction is maximum, and then it decreases again. In contrast, for the case of III studied just above, the π^*_{xz} orbital remains unchanged during the reaction. The HOMO of complex V is far lower than in III, and it mixes early with the next orbital **5**. This induces its sharp rise until it transforms into the HOMO of IX.

Even if the activation energy is higher from V than from III, the transition state derived from the former is more stable than that derived from the latter by 0.4 eV. It thus seems preferable to start from the most stable isomer V, although it appeared geometrically less favorable.

(c) Evolution of the Olefin π-Complex IX. As we said before, the Fe_a–olefin distance in IX is longer than usual in such complexes, indicating that the Fe–olefin interaction is less strong. Furthermore, the octahedral environment of the irons is distorted (see the α and β angles in X). Therefore, one can wonder whether IX would not easily open to give XIb, which by a rotation around Fe–Fe leads to the more stable conformer XIa. The arrangement of the ligands in XIa or XIb is the same as in V and is explained by the same arguments (see section IIa).

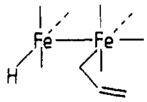

XIa

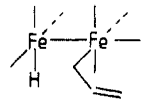

XIb

XIa has been computed to be 9 kcal/mol more stable than IX. The decomposition of both molecules into $Fe_2(CO)_7H$ and C_3H_5 fragments shows that the interaction between these two fragments is more stabilizing in IX than in XIb. This is due to the supplementary interaction of the double bond with Fe_a. However, the $Fe_2(CO)_7H$ fragment in XIb (XIIa) is far more stable than in IX (XIIb) for the same reason that VIII is more stable than VI. The interaction of the double bond with Fe_a is not strong enough to overcome this difference.

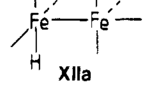

XIIa

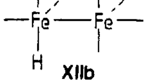

XIIb

The opening of IX to give XIb has a small energy barrier of 0.4 eV. It is essentially due to the orbitals having a bonding character between Fe_a and the double bond. However, their rise is rapidly canceled by the decrease of the HOMO that is $d_{x^2-y^2}$ on Fe_a and that is strongly stabilized by the creation of the vacant site along the x axis (see section IIa). Therefore, it seems likely that the olefin complex IX opens to XIb, which then gives XIa, having moreover a better geometry for a further reductive elimination.

XIa is unsaturated on Fe_a. Its evolution can follow various paths. First, it can recoordinate a CO to give the saturated complex XIII, for which the dinuclear reductive elimination will be studied. Our calculations show that no barrier exists for this CO coordination. Second, XIa can remain unsaturated. In this case, two possibilities can

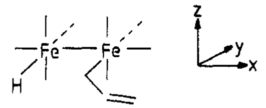

XIII

---

(23) (a) Caloron, H. J.; Hirota, E.; Kuchitsu, K.; Lafferty, W. J.; Maki, A. G.; Pote, C. S. *Structure Data of Free Polyatomic Molecules*; Landolt-Börnstein New Series, Group II; Springer-Verlag: Berlin, 1976; Vol. 7. (b) Davis, M. I.; Speed, C. S. *J. Organomet. Chem.* **1970**, *21*, 401. (c) Axe, F. U.; Marynick, D. S. *J. Am. Chem. Soc.* **1984**, *106*, 6230–6235.

be examined. The first one is that a dinuclear elimination also occurs. We will then compare this elimination on XIa and XIII in order to see if the CO coordination takes place before or after the elimination. The second possibility is the existence of fluxional processes (see section IVc).

(d) Dinuclear Reductive Elimination. We have already said in the Introduction that the intramolecular dinuclear [1 − 2] reductive elimination is an unfavorable reaction.[6] Since the carbon chain in XIII is allylic, we have investigated a process where the reductive elimination is accompanied by a rearrangement, giving a six-center transition state, with the hope that it will be more favorable (eq 4). In fact, this reaction looks like the ene reaction

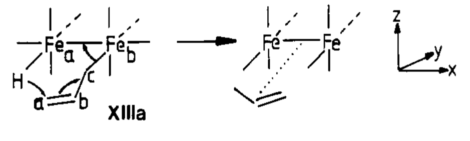

(4)

where pentene gives propene and ethylene through the cyclic transition state XIV. The endo products are formed

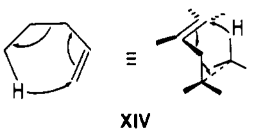

XIV

preferentially in agreement with the Woodward–Hoffmann rules.[24] The best starting conformation for this dinuclear reductive elimination is XIIIa, in which a torsion angle $C_bC_cFe_bFe_a$ of 70° has been chosen in order to approach H and C_a. This conformation is quasi-isoenergetic with the most stable one, XIII (2.5 kcal/mol above).

The $Fe_2(CO)_8$ conformation written is the best one found. However, it is not stable toward Fe–Fe dissociation: the Fe–Fe overlap population is 0.07, indicating that the bonding between the iron atoms is very weak. This is due to the fact that all the in-phase and out-of-phase orbital combinations are full when two $Fe(CO)_4$ fragments couple. The stable complex is $Fe_2(CO)_8^{2-}$.[25]

All structural parameters were varied linearly. The Fe–H and Fe–C bonds were stretched along the *y* direction and the carbon chain was rotated in order to finally bring C_a in the *xy* plane. The evolution of the most important orbitals during the reaction is shown in Figure 3. It is fundamentally a forbidden reaction, since a strong avoided crossing exists. The LUMO of XIII is Fe–H and Fe–C antibonding and C–H bonding. Thus, it decreases sharply when the Fe–H and Fe–C bonds are elongated and when H approaches C. The HOMO **10** is also Fe–H and Fe–C antibonding but is C–H antibonding. The two effects cancel at the beginning of the reaction. However, when **10** mixes with **11**, a large coefficient develops on the carbons, enhancing the C–H antibonding character (see **10a**). Moreover, the orbital on Fe_b becomes $p_x + p_y$ and is now Fe–C bonding. **10a** therefore rises rapidly, giving the avoided crossing with the LUMO.

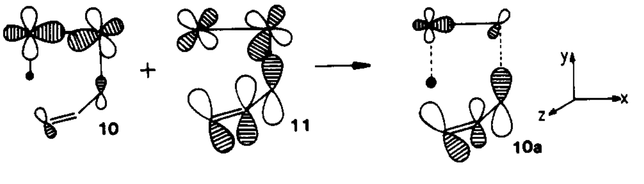

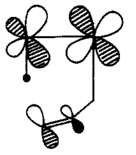

12

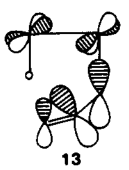

13

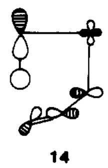

14

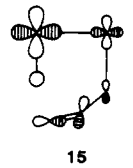

15

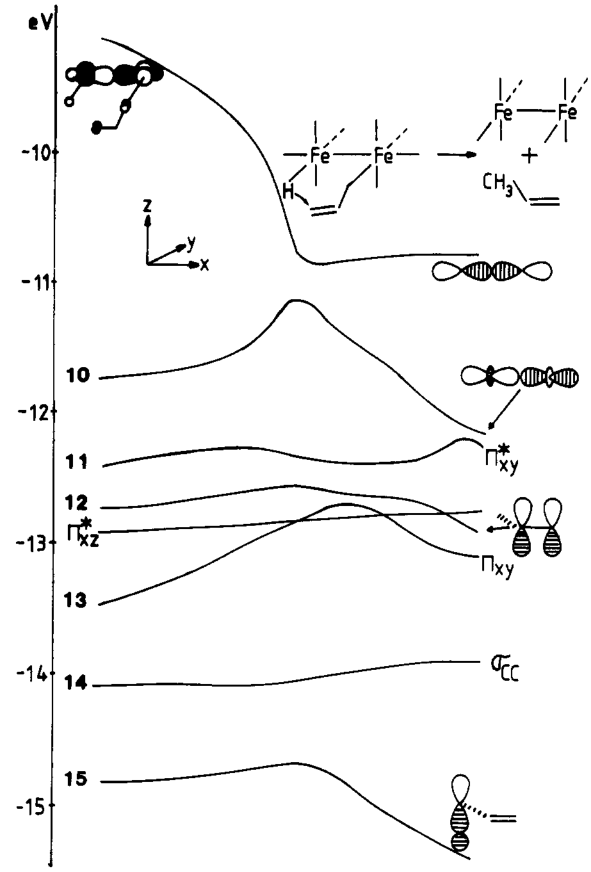

Figure 3. Evolution of the main orbitals during the dinuclear elimination involving a six-center transition state (eq 4). Orbitals 10–15 are drawn in the text.

Another interesting orbital that contributes greatly to the barrier is **13**. It is Fe–C and Fe–H bonding and C–H antibonding. It would correlate with the σ^*_{CH} orbital. However, owing to the lack of symmetry, its rise is stopped by successive mixing with upper orbitals. Finally there are two σ_{FeH} orbitals, **14** and **15**, both concentrated on H. Whey they mix together, **14** loses its coefficient on H and evolves smoothly to the σ_{CC} orbital of the propene while **15** evolves to the σ_{CH} orbital.

The computed energy is high: 3.4 eV. We have tried to improve it in various ways. It has been said previously that $Fe_2(CO)_8$ decomposes spontaneously to $Fe(CO)_4$. Thus, a pathway can be envisaged where the Fe–Fe bond breaks during the H migration. The LUMO and the HOMO of XIII are Fe–Fe antibonding and Fe–Fe bonding, respectively. When the Fe–Fe bond is elongated, the LUMO decreases and the HOMO rises earlier in the reaction. The result is that they also mix earlier and the HOMO begins to decrease before **13** or **15** reach their maximum. The energy barrier is thus lower: 3 eV. If now the Fe–H and Fe–C bonds are elongated more slowly at the beginning of the reaction, the energy barrier is diminished to 2.6 eV but the reaction remains symmetry forbidden.

In conclusion, the reaction path through a cyclic six-center transition state is not favorable. What is the difference with the ene reaction? Our transition state has

---

[24] Berson, J. A.; Wall, R. G.; Perlmutter, H. D. *J. Am. Chem. Soc.* **1966**, *88*, 187–188.

[25] Chin, H. B.; Smith, M. B.; Wilson, R. D.; Bau, R. *J. Am. Chem. Soc.* **1974**, *96*, 5285–5287.

the same geometry as that leading to the endo product in the ene reaction. In both reactions, the transition state can be viewed as made up of the combination of a hydrogen atom with a radical.[26] Let us examine the shape of the SOMO's **16** and **17** of these radicals.

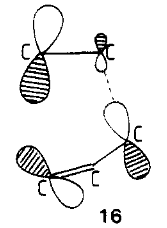

16

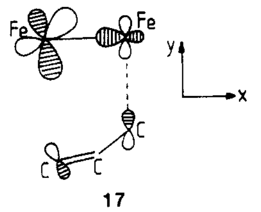

17

In **16** (ene reaction), the interacting hydrogen will be bonding with both carbons. In contrast, in the SOMO **17** of the dimetalla complex, the hydrogen will be bonding with Fe and antibonding with C. In both cases, the SOMO arises from the combination of the n allyl orbital of the CH_2CHCH_2 fragment in phase with the LUMO of the CH_2CH_2 or $Fe_2(CO)_8$ fragment and out of phase with the HOMO of these fragments:

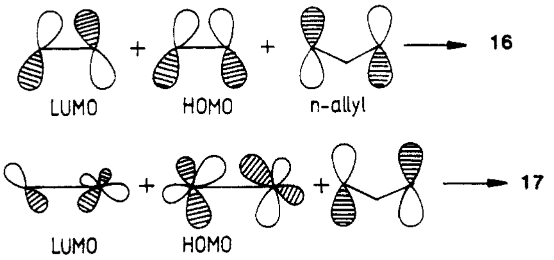

The CH_2CH_2 and $Fe_2(CO)_8$ fragments have a symmetry plane perpendicular to the C–C or Fe–Fe bond. Relative to this plane, the two LUMO's have an inverse symmetry, as do the two HOMO's. This explains the difference in the SOMO shape and consequently the difference in the behavior of the two systems.

We will now compare the previous mechanism with the more traditional dinuclear elimination already studied by Hoffmann for other systems[6] (eq 5). We have varied

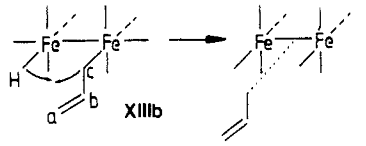

(5)

linearly all distances and angles in a reaction path looking like the C_{2v} pathway of ref 6. This time the starting complex is XIIIb, where the torsion angle $C_bC_cFe_bFe_a$ is 90°. It is quasi-isoenergetic with XIII. The carbon chain does not rotate as before, but H and C_c approach each other in the *xy* plane. In Figure 4 are plotted the energies of the most important orbitals. The interesting feature is the disappearance of the strong avoided level crossing that existed in Figure 3. The reaction is now allowed (smooth evolution of the C–H overlap population), but its energy barrier is still high (2.5 eV). The same series of mixing take place as before between orbitals **10**–**14**, giving avoided crossings. The difference lies in the behavior of orbital **10a**, which results from the mixing of **10** and **11** (see above). Since the coefficients on C_a and C_c are opposed, this time the mixing induces a bonding character between H and C_c and the HOMO **10** does not rise as it did in Figure 3. Therefore, its behavior prevents the existence of a strong avoided crossing.

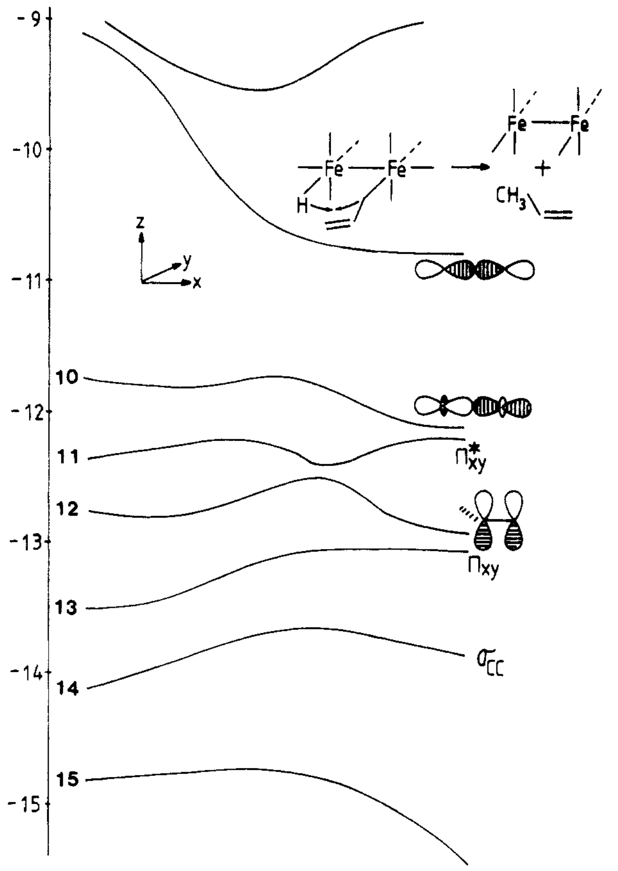

Figure 4. Evolution of the main orbitals during the dinuclear elimination given in eq 5. Orbitals **10**–**15** are drawn in the text.

Let us now compare our results with those of Hoffmann. Our system has no symmetry. The FeH and FeC orbitals lie at very different energies: the n allyl orbital is high in energy (–11.4 eV) and interacts strongly with the metallic fragment, giving **11**. In contrast, the H s orbital is low in energy (–13.6 eV) and gives the deep orbitals **14** or **15** with the metallic fragment. The result is that no orbital contains large coefficients both on H and on C. The bonding or antibonding character between H and C is thus smaller, and the orbital energies vary less sharply than in the symmetrical case. However, the orbital behavior is intrinsically the same: the out-of-phase combination of the metal–H bonds, which was responsible for the level crossing ($1b_2$ orbital), is in our system split into **13** and **14**, respectively more concentrated on FeC and FeH. They mix together, and then **13** mixes with the higher orbital **12** ($1b_2$–$2b_2$ avoided crossing in ref 6). However, the rise of **12** is hindered by a new avoided crossing with **11**, which in turn mixes with the HOMO **10**, whose behavior, as we have just seen, prevents the existence of a strong avoided crossing. This explains in part why the energy barrier that was 7.9 eV in Hoffmann's case is 2.5 eV for our system. In the dihydrido complex, orbital **11** does not exist. Consequently, even if the symmetry were artificially broken in order to avoid the level crossing, the energy barrier would be larger than for our system. In effect, no orbital could hinder the rise of **12** before it meets **10**. Let us now replace the allyl group by a methyl. The same reaction path has been computed. The orbital behaviors are similar to that described in Figure 4 and the energy barrier has the same order of magnitude (0.3 eV larger).

Therefore, it seems that the dinuclear reductive elimination is easier from a dissymmetric complex (elimination of alkyl-H for example) than from a dihydrido complex. Another reason for the smaller energy barrier in our system

---

[26] Hoffmann, R.; Woodward, R. B. *Science* **1970**, *167*, 825–831.

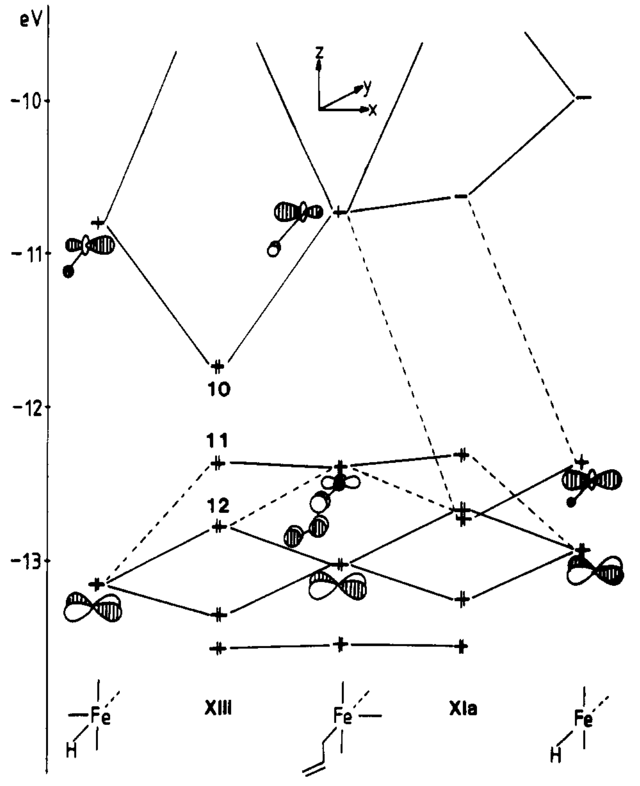

Figure 5. Interaction diagram between $Fe(CO)_4C_3H_5$ and $Fe(CO)_3H$ or $Fe(CO)_4H$ fragments.

comes from the position of the d orbitals of the metal used. Such a comparison between metals (Pd versus Ni) has been made in a study of reductive elimination on mononuclear complexes.[10] The two elimination reactions, mono- and binuclear have a common point: the antibonding b_2 orbital responsible for the energy barrier evolves to a metal d orbital. Therefore, the same conclusion holds: the lower the d level, the lower the barrier. The Fe d orbitals are lower than those of manganese, which was the metal studied by Hoffmann in the dinuclear elimination (-12.7 vs -11.67 eV). Consequently, this reaction would be easier for iron complexes than for manganese complexes. Finally, in this reaction path, the breaking of the Fe-Fe bond increases the energy barrier. This time, the barrier does not depend on the LUMO-HOMO mixing and it is unfavorable that the HOMO rises too high.

Let us now study the dinuclear reductive elimination on the unsaturated complex XIa. The interaction diagrams between the $Fe(CO)_4C_3H_5$ fragment on one hand and $Fe(CO)_4H$ or $Fe(CO)_3H$ on the other hand are described in Figure 5. They give the correspondence between the orbitals of XIa and XIII. The main feature is the lowering of the $Fe(CO)_3H$ SOMO (d_{z^2}) relative to the $Fe(CO)_4H$ SOMO due to the lack of CO on the x axis. The interaction with the SOMO of $Fe(CO)_4C_3H_5$ that results gives a low-lying orbital that is no longer the HOMO of the resulting complex. The other orbitals are not changed. The HOMO is now **11**. We have seen before that it mixed with **10** and **12**. Now the mixing with **10** does not exist any more: the coefficient on C_c does not diminish and nothing hinders **11** from rising quickly. The energy barrier is 0.5 eV higher than from XIII. Therefore, it is preferable to recoordinate CO on XIa before the reductive elimination occurs.

In conclusion, the two steps of path a (β-hydride elimination and dinuclear elimination) are allowed but their activation energy is rather high (2.3 and 2.5 eV, respectively).

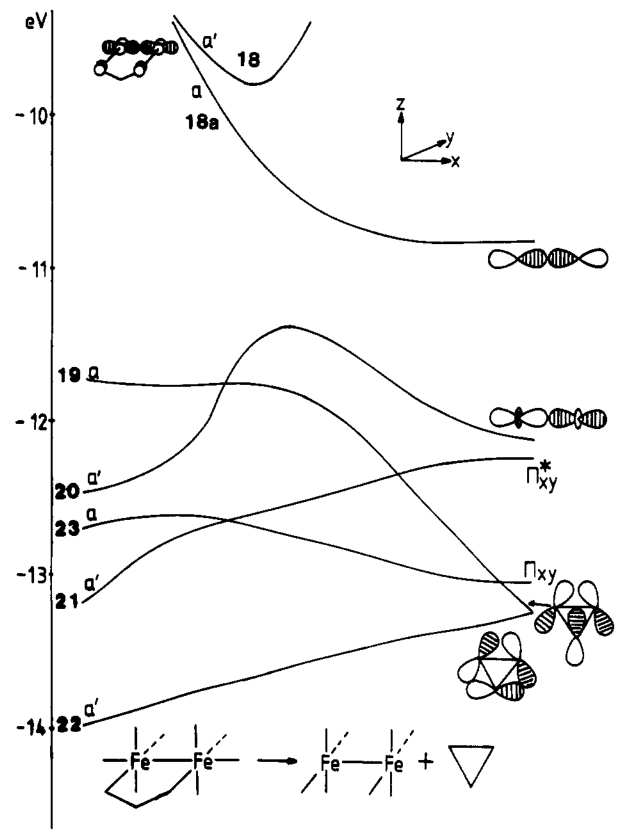

Figure 6. Evolution of the main orbitals during the transformation of I into cyclopropane. Orbitals **18**-**23** are drawn in the text.

III. Reaction Path Leading to Cyclopropane (Path c)

Since we were just speaking of dinuclear elimination, we will now consider the reaction leading to cyclopropane from I (eq 6). Initially, all distances and angles were varied

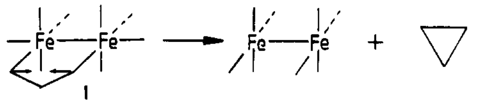

I

(6)

linearly and the symmetry plane, perpendicular to Fe-Fe at its middle point, was preserved throughout the reaction (C_s symmetry). The orbital energies are plotted in Figure 6. The curves are similar to those obtained by Hoffmann in ref 6, but no HOMO-LUMO crossing occurs and the energy barrier is far lower (2.9 eV). Two reasons are behind this different behavior: first, the position of the Fe d orbitals, and second, the fact that we have metal-C instead of metal-H bonds. If we exclude orbital **22**, which is concentrated on the carbon chain and evolves smoothly

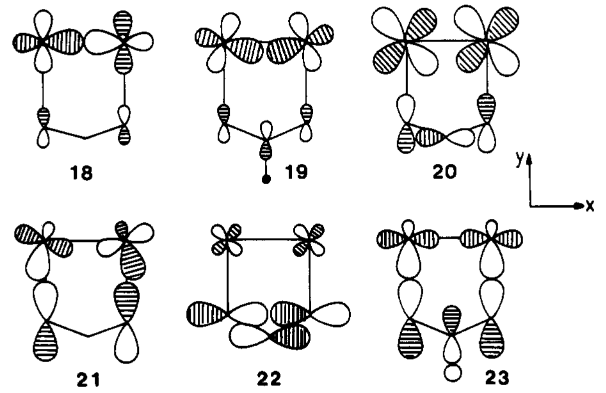

to one of the degenerate orbitals of cyclopropane, the orbital implicated in the barrier height is **21** (Fe–C bonding and C–C antibonding). It is higher in energy than the $1b_2$ orbital of ref 6 because it implies Fe–C bonds. In contrast, orbitals **20** and **18**, which are more concentrated on the metals, are lower than in ref 6 owing to the position of the Fe d orbitals. Thus, the successive crossings **21** with **20** and **20** with **18** (the $1b_2$–$2b_2$ and $2b_2$–$3b_2$ crossings of ref 6, respectively) occur earlier in the reaction, and this hinders **20** to go too high and to cross the LUMO **18a**. The breaking of the Fe–Fe bond only slightly decreases the barrier to 2.8 eV. We have also tried to suppress all symmetry by rotating the cyclopropane formed around the axis joining the middles of Fe–Fe and C_a–C_c. The barrier is also only slightly decreased to 2.7 eV, although **20** no longer crosses **19**. Its lowering is canceled by the rise of other orbitals due to the rotation.

In conclusion, the elimination of cyclopropane from a diferracyclopentane has a large barrier (2.7 eV) but is not impossible in comparison with the β-hydride elimination, whose barrier is 2.3 eV.

IV. H Migration with FeC and FeFe Cleavage (Path b). Mononuclear Reductive Elimination

(a) H Migration. We will now study the pathway where the migrating hydrogen is set on the iron atom to which the carbon chain remains bound (path b). In this way we obtain the hydrido–alkyl complex XV (eq 7), which can further lead to propene by a mononuclear reductive elimination. A problem arises in the structure of $Fe(CO)_4$. At the EHT level, the results are conflicting between the D_{2d}, D_{4h}, and C_{2v} geometries.[11b,27] With our parameters and our bond lengths we have found the D_{4h} geometry to be the best. Experimentally, however, $Fe(CO)_4$ has been shown to be paramagnetic. Effectively ab initio calculations[28] show that the triplet state with C_{2v} geometry is the most stable. In any event, $Fe(CO)_4$ will be trapped at once by ethylene. Therefore, the singlet state is to be considered.

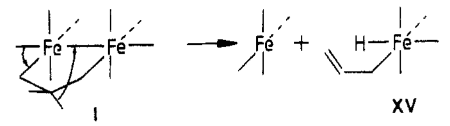

(7)

As for the preceding pathways, the geometrical parameters are varied linearly and the orbital evolutions are plotted in Figure 7. A strong avoided crossing exists: the reaction is symmetry forbidden and its energy barrier is high (3.1 eV).

In contrast with the case studied above (Figure 6), there is no symmetry and the vacant orbitals **18** and **18a** mix together, giving **18b**, which is Fe_a–C_a and Fe_a–Fe_b antibonding. When these two bonds are broken, the LUMO's energy decreases sharply. The HOMO **19** is, in contrast, Fe–Fe bonding. Furthermore, as we said in a preceding section (IIb), a rotation occurs around C_b during the reaction. A coefficient appears on H_b, bonding with C_b and therefore antibonding with Fe_b. The HOMO rises quickly. The foregoing explains the avoided crossing.

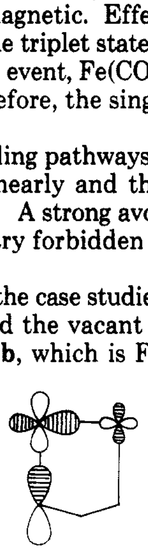

18b

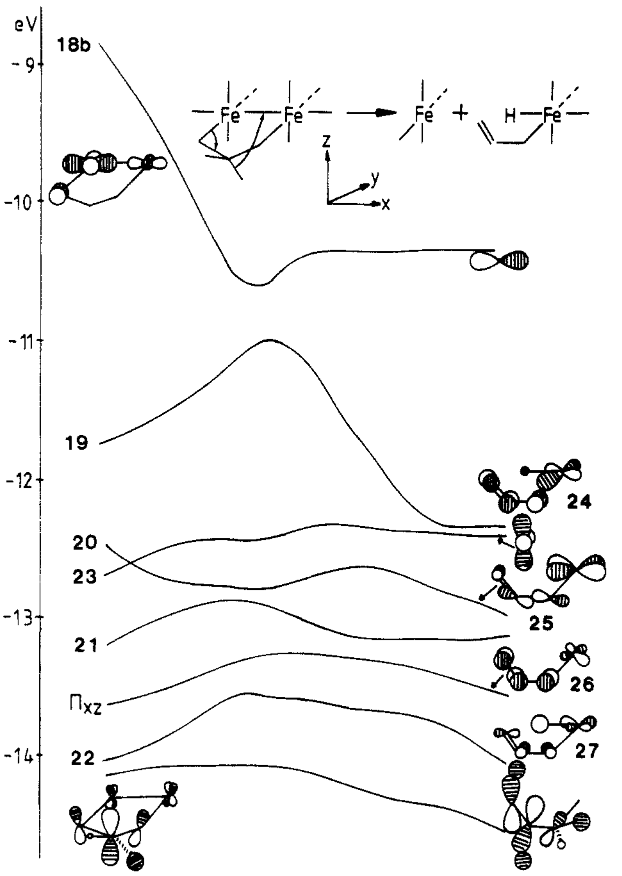

Figure 7. Evolution of the main orbitals for eq 7: I → XV.

As in section II, the other orbitals give rise to a sequence of avoided crossings. For example, the low-lying $\sigma_{C_bH_b}$ orbital mixes with **22**, owing to the movement of H_b and the rotation of the carbon chain. It loses its H_b character and evolves to a combination of the σ_{CH} bonds. In contrast, **22** acquires a large coefficient on H_b bonding with C_b and evolves after rising to a Fe_bH bonding orbital.

(b) Reductive Elimination. Reaction 7 leads to the cis hydrido–alkyl complex XV, which by reductive elimination can yield propene. The reductive elimination of alkane has been theoretically studied for d^8 transition-metal centers such as Ni(II), Pt(II), Pd(II), and Au(III).[10] For comparison, we have computed the same reaction path, as shown in eq 8. The angles COFeCO and HFeC are varied linearly, as is the angle α between the pseudo-3-fold axis of the CH_2C group and the Fe–C bond. The Fe–H and Fe–C bonds are elongated with increasing steps. The evolution of the energy levels is shown in Figure 8: the reaction is symmetry-allowed. The same facts as before are observed, when we compared our results with those of Hoffmann for the dinuclear elimination: since the FeH and FeC orbitals do not have the same energy and since the allyl group has more orbitals than CH_3, our system has more orbitals involved in the reaction, but their behavior is intrinsically the same as in Hoffmann's work. The totally bonding orbital (a_1 in ref 10) is **28**. However, it does

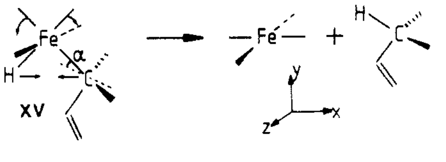

(8)

---

(27) Burdett, J. K. *J. Chem. Soc., Faraday Trans. 2* **1974**, *70*, 1599. Pensak, D. A.; McKinney, R. J. *Inorg. Chem.* **1979**, *18*, 3407.

(28) Daniel, C.; Benard, M.; Dedieu, A.; Wiest, R.; Veillard, A. *J. Phys. Chem.* **1984**, *88*, 4805–4811.

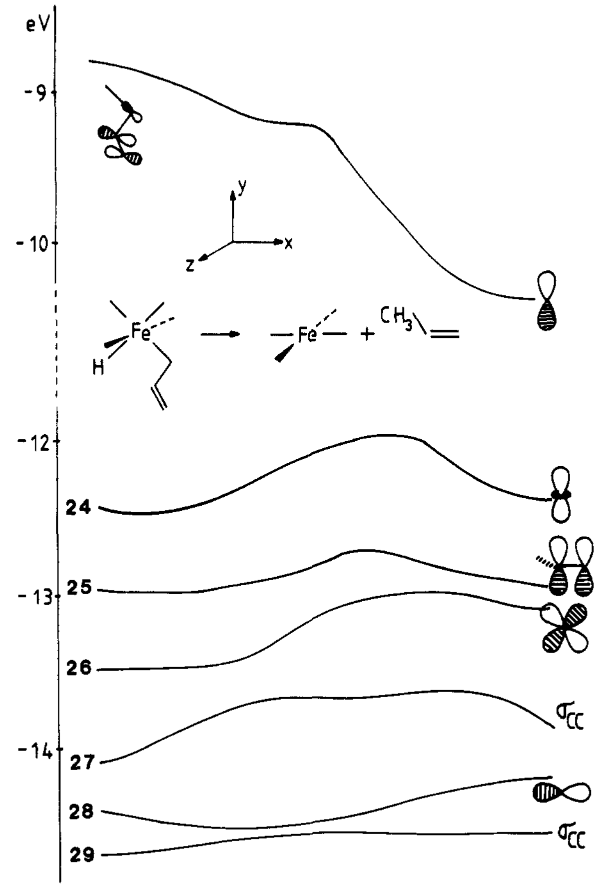

Figure 8. Evolution of the main orbitals during the reductive elimination given in eq 8. Orbitals **24**–**29** are drawn in the text.

not evolve to the σ_{CH} bond, owing to a crossing with the deeper orbital **29**.

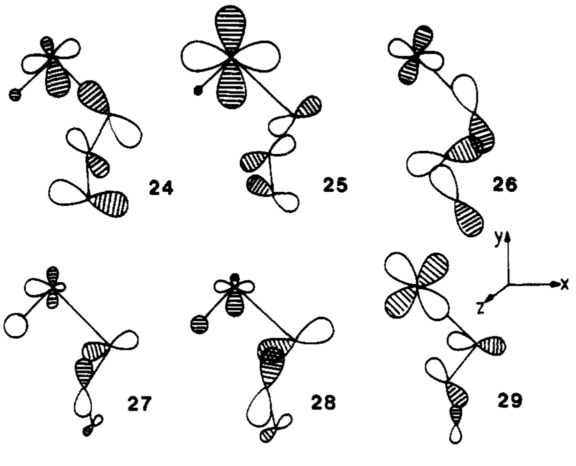

The orbital bonding between Fe and H or C but antibonding between H and C (b_2 orbital in ref 10) in **27**. It would rise sharply but, as in the case of the dinuclear elimination, a sequence of avoided crossings arises until the HOMO **24**. This latter orbital is Fe–C and C–H bonding and Fe–H antibonding. When it mixes with **25** early in the reaction, it gives **24a**, where first the bonding Fe–C character predominates, inducing its rise. However, H and C rapidly approach each other, the CH bonding character prevails, and **24** decreases without going very high in energy.

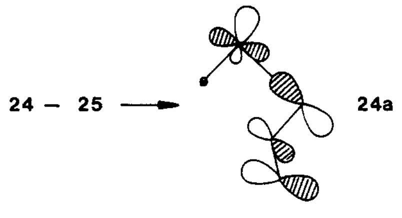

Therefore, the reductive elimination from our d^6 complex is symmetry allowed. The computed activation energy is 2.3 eV. This is in agreement with Hoffmann, who said that the eliminations from planar d^8 and octahedral d^6 complexes must have the same energy profiles. Our energy barrier is a little smaller than his. This could be due to the lack of symmetry in our system and to the relative energy of the d orbitals on Fe and Pd (same conclusion as for the dinuclear elimination). The barrier can even be reduced to 2 eV by using a geometry that keeps H near Fe for a longer time.

Hoffmann also pointed out that the reductive elimination is easier from a three-coordinate than from a four-coordinate d^8 complex because the two L ligands in ML_2R_2 destabilize the b_2 orbital. In the same way, elimination must be easier from a five-coordinate than from a six-coordinate d^6 complex. We have verified this assumption by studying the reductive elimination from $Fe(CO)_3H(C_3H_5)$ (XVI). Several isomers can be considered. It has

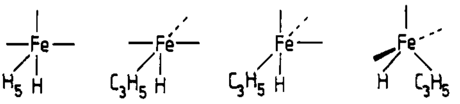

XVIa XVIb XVIc XVId

been shown that a d^6 ML_5 complex prefers the square-planar pyramidal geometry[11b] with the stronger σ donor in the apical position.[11a]

Effectively, XVIa is more stable than XVIb, XVIc, and XVId by 0.3, 0.5, and 1 eV, respectively (the allyl C_3H_5 is a better σ donor than the hydride). XVId is the isomer corresponding to the MLR_2 complex studied by Hoffmann. The reductive elimination from XVId, computed with the same geometrical parameters as in eq 8, has an energy barrier of only 1 eV (compared with 2.3 eV). If the starting point is the most stable isomer XVIa, with a CO rotation in the HFeC plane (eq 9), the lowering of the barrier is only

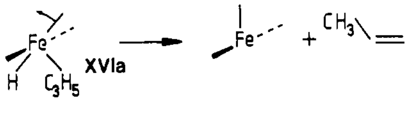

(9)

0.35 eV because in this isomer the ligand has the same position as in XV at the beginning of the reaction. Finally, the transition states from XVIa and XVId are isoenergetic. With a geometry that does not break Fe–H too quickly, the barrier is reduced to ca. 1.7 eV.

In conclusion, the mononuclear reductive elimination has a smaller energy barrier than the dinuclear reductive elimination because it is intrinsically symmetry allowed, whereas the latter reaction is intrinsically forbidden and becomes allowed only by the lack of symmetry. Furthermore, the mononuclear elimination is easier from a five-coordinate than from a six-coordinate d^6 complex. The above result leads us to search for a way to obtain the cis hydrido–alkyl complex XVI by an allowed reaction (see the next section).

(c) Fluxional Behavior of XIa. It is well-known that, in solution, dinuclear complexes can display a fluxional behavior, i.e. an interconversion of bridged and terminal ligands at relatively low temperature.[25,29] The energy

---

(29) Cotton, F. A.; Hanson, B. E.; Jamerson, J. D.; Stults, B. R. *J. Am. Chem. Soc.* **1977**, *99*, 3293–3257. Adams, R. D.; Cotton, F. A. *J. Am. Chem. Soc.* **1973**, *95*, 6589–6594.

Scheme III

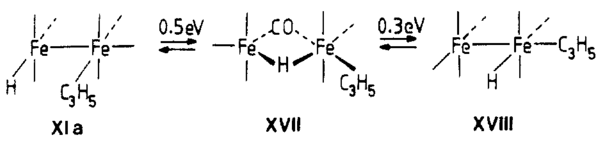

barrier would be on the order of 10 kcal/mol (0.4 eV) or even less. Earlier calculations show that opening or breaking two bridges in a d^7–d^7 system is symmetry allowed.[30] Furthermore, some thermodynamic data suggest an energetic preference for bridging over terminal Fe–H bonds.[31] Owing to the foregoing and the fact that XIa is a dissymmetric unsaturated complex, we have envisaged the sequence of the equilibria shown in Scheme III.

The energy barriers are low (respectively 0.5 and 0.3 eV) compared to all that have been found for the various reactions studied. XVII is slightly more stable than XI (0.1 eV), but XVIII is the most stable $Fe_2(CO)_7H(C_3H_5)$ isomer calculated in this work. This is due to the apical position of the strong σ-donor allyl ligand, as already mentioned. A consequence of this position is the weakening of the Fe–Fe bond: the overlap population, which is 0.14 in XI, is reduced to 0.11 in XVIII, owing to the large donation of the σ allyl orbital into the σ^* FeFe orbital, which is the LUMO of the $Fe_2(CO)_7H$ fragment. Remember that the FeFe overlap population in the unstable $Fe_2(CO)_8$ complex is 0.07. Therefore, XVIII would dissociate easily, giving $Fe(CO)_4$ and XVIa. The reaction is slightly endothermic and requires no barrier. It is even more favorable to start from XVII, which evolves smoothly to $Fe(CO)_4$ and XVIa without any barrier by an exothermic path (breaking of the bridges without re-forming the Fe–Fe bond). In conclusion, the migration of the hydride from one iron atom to the other (Scheme III), followed by the cleavage of the Fe–Fe bond, is an easy way to obtain a complex favorable to a further mononuclear elimination.

V. H Migration to the Carbon (Path d, Scheme II)

Let us now study the last mechanism envisaged in the Introduction. The two Fe–C bonds being broken during this reaction, one obtains a system similar to the trimethylene diradical:

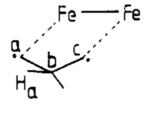

This diradical has been postulated to be an intermediate in the isomerization of cyclopropane to propene.[32] In fact, this mechanism has been debated and theoretical calculations have shown that the reaction is concerted.[33] To our knowledge, no detailed theoretical study has been made on the conversion of the trimethylene diradical to propene, for which thermodynamic calculations have given an activation energy of 11 kcal/mol.[34] This reaction can be considered as a 1,2-sigmatropic migration of hydrogen in a radical (isomerization of a primary to a secondary radical). Two electrons are involved, and by the symmetry rules,[35] the reaction is suprafacial. In agreement, our calculations show that no barrier occurs in the migration of H_a from C_b to C_a. The total lack of barrier could come from the starting geometry: the trimethylene diradical has the same geometry as the carbon chain in complex I, and therefore, the $C_cC_bC_a$ angle is greater than in the ab initio optimized geometry[36] and is roughly equal to 120° as in propene.

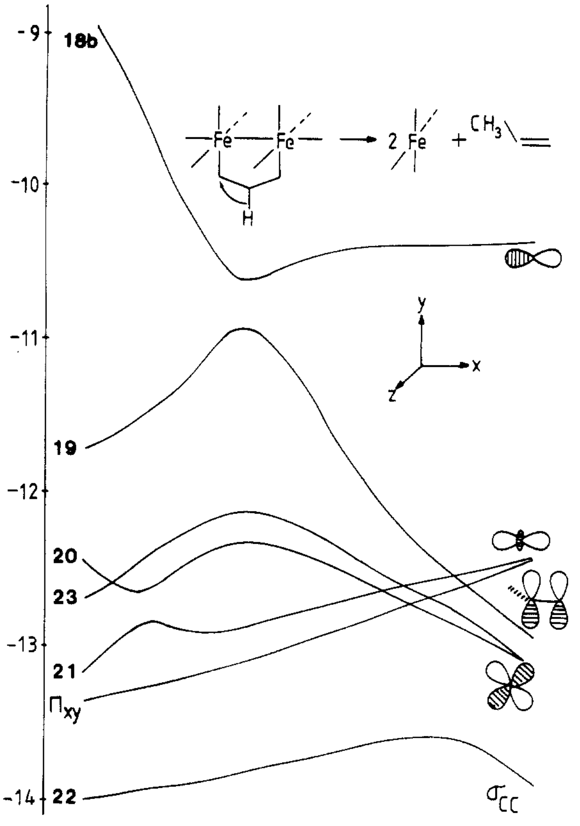

Figure 9. Evolution of the main orbitals during the H migration to the carbon (path d).

What does happen when the same reaction is considered in complex I (Scheme II)? First, we have established that it is more favorable to also break the Fe–Fe bond as in section IIb. The reason is the same: the transition state is reached earlier along the reaction path. The orbital evolution is shown in Figure 9. An avoided crossing occurs: the reaction is forbidden. The migrating H is now H_a, and the $\sigma_{C_bH_a}$ bond appears in orbitals **19** and **23**. The HOMO **19** is Fe–Fe and C_b–H_a bonding but C_a–H_a antibonding. It rises sharply, even though it is Fe–C antibonding. In contrast, the LUMO **18** is Fe–Fe and Fe–C antibonding and decreases rapidly when these bonds are broken. This explains the avoided crossing between the frontier orbitals. Orbital **23** also contributes strongly to the barrier height: it is Fe–Fe, Fe–C, and C_b–H_a bonding but C_a–H_a antibonding. It would correlate with the $\sigma^*_{C_aH_a}$ orbital, but as in the preceding pathways, its rise is stopped by avoided crossings.

The computed barrier is high (3.5 eV). We can decompose it in two parts: the energy required for breaking the bonds up to the transition state and then the energy required for the H migration. The former has been computed to be 2.6 eV. There remains 0.9 eV for the latter, whereas no barrier has been found for the H migration in the trimethylene diradical itself. This difference comes

---

[30] Jemmis, E. D.; Pinhas, A. R.; Hoffmann, R. *J. Am. Chem. Soc.* **1980**, *102*, 2576–2585.

[31] Vites, J.; Fehlner, T. P. *Organometallics* **1984**, *3*, 491–493.

[32] Trautz, M.; Winkler, K. *J. Prakt. Chem.* **1922**, *104*, 53. Chambers, T. S.; Kistiakowsky, G. B. *J. Am. Chem. Soc.* **1934**, *56*, 399.

[33] Jug, K. *Theor. Chim. Acta* **1976**, *42*, 303–310.

[34] Benson, S. W. *J. Chem. Phys.* **1961**, *34*, 521.

[35] Woodward, R. B.; Hoffmann, R. *J. Am. Chem. Soc.* **1965**, *87*, 2511–2513.

[36] Kato, S.; Morokuma, K. *Chem. Phys. Lett.* **1979**, *65*, 19–25.

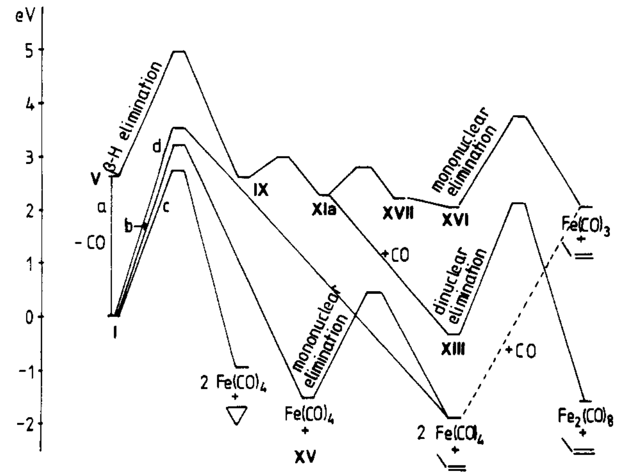

Figure 10. Relative energies of the transition states for the various pathways.

from an inversion of the orbitals when the trimethylene diradical interacts with the $Fe_2(CO)_8$ fragment (see Figure 4 in ref 1): the LUMO of the trimethylene diradical is now partly the HOMO of the complex, and its HOMO becomes, in contrast, the LUMO of the complex. When the Fe–C bonds are stretched, the first situation is gradually reached again but not soon enough to avoid an activation energy. In conclusion, the presence of the metals makes the 1,2-migration more difficult.

VI. Conclusion

The various reaction paths studied in this work are summarized in Figure 10. The starting complex I is taken as the energy reference. At this point, we must keep in mind that the method used cannot give quantitative results, especially for reactions involving bond making and breaking. However, since in all reaction paths the same bonds are made or broken, we can compare the computed activation energies meaningfully, as their magnitudes reflect the orbital evolutions. The only reaction that cannot be compared to the others is the CO dissociation. Now the conclusions of this work rest on the energy needed for this dissociation.

Three reactions have been found to be symmetry allowed: β-hydride elimination, mononuclear cis reductive elimination, and dinuclear reductive elimination. The last reaction has the greatest activation energy because it is in fact intrinsically forbidden and becomes allowed only by lack of symmetry.

In consequence, if the CO dissociation is easy, the best reaction path is the following: a prior CO dissociation and a β-hydride elimination lead to the unsaturated dinuclear hydrido–alkyl complex $Fe(CO)_3HFe(CO)_4(C_3H_5)$. By easy fluxional movements, the hydride is transferred from one Fe to the other with the breaking of the Fe–Fe bond and the mononuclear cis hydrido-alkyl complex $Fe(CO)_3H(C_3H_5)$ is obtained. A reductive elimination then yields the products.

If the CO dissociation is difficult, the reaction will have a large energy barrier, since all the mechanisms calculated in this case are forbidden. Among them, the easiest is the formation of cyclopropane. If the energy barriers of the cyclopropane formation and of the CO loss are on the same order of magnitude, the two reactions are competitive and a mixture of propene and cyclopropane is obtained. If the CO loss is totally inhibited, the only product is cyclopropane. These results are in agreement with the experimental data described in the Introduction.

VII. Appendix

All calculations were performed by using the extended Hückel method[37] with weighted H_{ij}'s. The values for the H_{ii}'s and exponents are taken from previous works (ref 38 for example). The following bond distances were used: Fe-Fe = 2.72 Å in the dimetallacycles and 2.85 Å in the noncyclic compounds, Fe–CO = 1.82 Å, C–O = 1.15 Å, Fe–H = 1.6 Å, Fe–C = 2.15 Å, C–C = 1.34 Å (double bond), C–C = 1.52 Å (single bond adjacent to a double bond).

---

(37) Hoffmann, R. *J. Chem. Phys.* **1963**, *39*, 1397–1412.

(38) Eisenstein, O.; Hoffmann, R. *J. Am. Chem. Soc.* **1981**, *103*, 4308–4320.